

Structure of boson systems beyond the mean-field

O. Sørensen §, **D. V. Fedorov**, and **A. S. Jensen**

Department of Physics and Astronomy, University of Aarhus, DK-8000 Aarhus C,
Denmark

Abstract. We investigate systems of identical bosons with the focus on two-body correlations. We use the hyperspherical adiabatic method and a decomposition of the wave function in two-body amplitudes. An analytic parametrization is used for the adiabatic effective radial potential. We discuss the structure of a condensate for arbitrary scattering length. Stability and time scales for various decay processes are estimated. The previously predicted Efimov-like states are found to be very narrow. We discuss the validity conditions and formal connections between the zero and finite-range mean-field approximations, Faddeev-Yakubovskii formulation, Jastrow ansatz, and the present method. We compare numerical results from present work with measurements and mean-field calculations.

PACS numbers: 31.15.Ja, 05.30.Jp, 21.65.+f

Submitted to: *J. Phys. B: At. Mol. Phys.*

1. Introduction

The interest in dilute Bose gases has been growing since the experimental realisation of the phenomenon of Bose-Einstein condensation (BEC) [1, 2, 3]. Excellent reviews of the world of BEC are given in recently published monographs [4, 5].

The theoretical interest in BEC goes more than fifty years back and is widely based on the mean-field formulation. The usual measure of the validity of the mean-field is that $n|a_s|^3 \ll 1$, where n is the density and a_s is the two-body s -wave scattering length [4]. Then the particles are not too close to each other and correlations are expected to be negligibly small as assumed in the mean-field approximation. The importance of correlations must increase with the density of the system and the mean-field method sooner or later becomes inadequate.

A Feshbach resonance is routinely used to create Bose-Einstein condensed systems where the effective interaction corresponds to a large scattering length a_s [6]. Then stronger correlated structures arise and the condensate becomes unstable as seen experimentally [7]. A theoretical description based on the time-dependent Gross-Pitaevskii equation (zero-range two-body interaction) was given in [8, 9]. By definition

§ To whom correspondence should be addressed (oles@phys.au.dk)

then only average properties are incorporated although the dominating decay mechanism is very sensitive to correlations.

The need to account for correlations seems unavoidable in experiments where clusterizations occur. The simplest example is probably the three-body recombination process, where two of the atoms in the many-body system react and form a two-body bound state. In [10] is suggested to apply a Feshbach resonance to create a hybrid atomic-molecular Bose-Einstein condensate. The atom-molecule coupling is included on top of the usual mean-field equations. It is then conjectured, that the ground state of a Feshbach resonant Bose-Einstein condensate in reality is a mixed condensate of atoms and di-atomic molecules. This type of mixed condensate was observed experimentally in [11]. There the structure of the molecules is discussed, but whether a molecular Bose-Einstein condensate is formed remains an open question.

Descriptions of correlations within N -body systems almost inevitably must employ few-body techniques which by definition are tools to understand the few-body structures decoupled from all other degrees of freedom. This immediately suggests to extend the use of suitable three-body formulations. A particularly promising set of calculations were reported in [12] for an isolated three-body system with total angular momentum zero. They varied the scattering length and described systems with any number of bound two-body states. Moreover, they studied a range of excited states and concluded that such higher-lying condensate-like states do not collapse under the usual conditions when $N|a_s|/b_t > 0.5$ [13], where b_t is the trap length of an external harmonic field.

Generalizations of this work to N -body systems were initiated in [14], where average properties of Bose-Einstein condensates were investigated by use of hyperspherical coordinates. In [15, 16] this adiabatic hyperspherical method was extended to include two-body correlations in N -body boson systems. The initial application for $N = 20$ was soon extended to particle numbers as high as 10^5 [17]. Systematic scaling properties are deduced as function of scattering length and particle number and analytic expressions are derived for the adiabatic potentials.

The results from [15, 16, 17] strongly indicate that the mean-field properties for dilute systems are reproduced in addition to the two-body correlations initially in focus. A better understanding of validity conditions and connections between mean-field models and the adiabatic hyperspherical expansion method are then desirable. Of particular interest are the correlations in systems with large scattering lengths which cannot be studied by mean-field methods.

The purpose of this article is to discuss both qualitative and quantitative gross properties of correlated N -body boson systems. It is then natural to compare with results from mean-field methods and other formulations to describe correlations. In section 2 we summarize the hyperspherical theory for studying correlations beyond the mean-field. In section 3 we present general properties of the hyperspherical potentials. In section 4 we discuss relations to the mean-field, improvements over the mean-field, and ranges of validity of both the mean-field and the present hyperspherical method. Finally, section 5 contains our conclusion.

2. Theory

We study N identical bosons of mass m trapped by an external harmonic field of angular frequency ω and interacting via a short-range interaction V . The Hamiltonian is then given by

$$\hat{H} = \sum_{i=1}^N \left(\frac{\hat{p}_i^2}{2m} + \frac{1}{2}m\omega^2 r_i^2 \right) + \sum_{i < j}^N V(r_{ij}) , \quad (1)$$

where \vec{r}_i is the position of particle i , \vec{p}_i the conjugate momentum, and $r_{ij} = |\vec{r}_j - \vec{r}_i|$ is the interparticle distance. The interaction part is independent of the center of mass. Both the kinetic energy and the external harmonic field can easily be separated into parts depending on the center of mass and parts only depending on relative coordinates. For this we use the relation

$$\sum_{i=1}^N r_i^2 = \frac{1}{N} \sum_{i < j}^N r_{ij}^2 + NR^2 , \quad (2)$$

where $\vec{R} = \sum_i \vec{r}_i / N$ is the center of mass coordinate. This immediately leads to the convenient definition of the hyperradius ρ

$$\rho^2 \equiv \frac{1}{N} \sum_{i < j}^N r_{ij}^2 = \sum_{i=1}^N r_i^2 - NR^2 . \quad (3)$$

Following this thread we choose a new set of coordinates, the hyperspherical coordinates, to describe the $3N - 3$ relative degrees of freedom. The hyperradius ρ sets the overall length scale for the system, and the relative orientations of the particles are determined by $3N - 4$ hyperangles Ω [18, 19]. One hyperangle $\alpha_{ij} \in [0, \pi/2]$ is related to the distance between two particles $r_{ij} \equiv \sqrt{2}\rho \sin \alpha_{ij}$.

2.1. Adiabatic hyperspherical method

The Hamiltonian then separates into a center of mass part, a radial part, and an angular part depending respectively on \vec{R} , ρ , and Ω [19]

$$\hat{H} = \hat{H}_{\text{c.m.}} + \hat{H}_\rho + \frac{\hbar^2 \hat{h}_\Omega}{2m\rho^2} , \quad (4)$$

$$\hat{H}_{\text{c.m.}} = \frac{\hat{p}_R^2}{2Nm} + \frac{1}{2}Nm\omega^2 R^2 , \quad (5)$$

$$\hat{H}_\rho = \hat{T}_\rho + \frac{1}{2}m\omega^2 \rho^2 , \quad (6)$$

$$\frac{\hbar^2 \hat{h}_\Omega}{2m\rho^2} = \hat{T}_\Omega + \sum_{i < j}^N V(r_{ij}) , \quad (7)$$

where \hat{T}_ρ and \hat{T}_Ω are related kinetic energy operators. The relative wave function $\Psi(\rho, \Omega)$ obeys the Schrödinger equation

$$(\hat{H} - \hat{H}_{\text{c.m.}}) \Psi(\rho, \Omega) = E \Psi(\rho, \Omega) . \quad (8)$$

The adiabatic expansion of the wave function is

$$\Psi(\rho, \Omega) = \sum_{\nu=0}^{\infty} F_{\nu}(\rho) \Phi_{\nu}(\rho, \Omega) , \quad F_{\nu}(\rho) = \rho^{-(3N-4)/2} f_{\nu}(\rho) \quad (9)$$

where Φ_{ν} is an eigenfunction of the angular part of the Hamiltonian with an eigenvalue $\hbar^2 \lambda_{\nu}(\rho) / (2m\rho^2)$

$$\hat{h}_{\Omega} \Phi_{\nu}(\rho, \Omega) = \lambda_{\nu}(\rho) \Phi_{\nu}(\rho, \Omega) . \quad (10)$$

Neglecting couplings between the different ν -channels yields the radial eigenvalue equation for the eigenfunction f_{ν} and the energy E_{ν}

$$\left(-\frac{\hbar^2}{2m} \frac{d^2}{d\rho^2} + U_{\nu}(\rho) - E_{\nu} \right) f_{\nu}(\rho) = 0 , \quad (11)$$

$$\frac{2mU_{\nu}(\rho)}{\hbar^2} = \frac{\lambda_{\nu}}{\rho^2} + \frac{(3N-4)(3N-6)}{4\rho^2} + \frac{\rho^2}{b_t^4} , \quad (12)$$

where $b_t \equiv \sqrt{\hbar/(m\omega)}$ is the trap length and the adiabatic potential U_{ν} is a function of the hyperradius. It consists of three terms, i.e., the external field, the generalized centrifugal barrier, and the angular average of the interactions and kinetic energies. The neglected non-diagonal terms are typically about 1% of the diagonal terms for attractive Gaussian potentials. Thus, the center of mass motion is separated out and the hyperspherical adiabatic method is promising simply due to small coupling terms. The remaining problem is the determination of the angular potential λ from the angular eigenvalue equation.

2.2. The wave function

We have so far not assumed specific structures or in any other way restricted the allowed Hilbert space for the many-body wave function. At some point we can not avoid to make a suitable ansatz for the angular wave function $\Phi_{\nu}(\rho, \Omega)$. However, first we shall study the historically successful approaches to a many-body wave function.

2.2.1. The Hartree mean-field description. The ground-state Hartree product of single-particle amplitudes [20]

$$\Psi_H(\vec{r}_1, \vec{r}_2, \dots, \vec{r}_N) = \prod_{i=1}^N \psi_{s.p.}(\vec{r}_i) , \quad (13)$$

is for the non-interacting gas in the external field given by

$$\psi_{s.p.}(\vec{r}_i) = C e^{-r_i^2/(2b_t^2)} , \quad C^{-1} = \pi^{3/4} b_t^{3/2} . \quad (14)$$

With the relation $\sum_{i=1}^N r_i^2 = \rho^2 + NR^2$ this can be rewritten as

$$\begin{aligned} \Psi_H(\vec{r}_1, \vec{r}_2, \dots, \vec{r}_N) &= C^N \exp \left[- \sum_{i=1}^N r_i^2 / (2b_t^2) \right] \\ &= C^N e^{-\rho^2/(2b_t^2)} e^{-NR^2/(2b_t^2)} = \Upsilon_0(\vec{R}) F_0(\rho) \Phi_0 . \end{aligned} \quad (15)$$

The separation of the center of mass motion assures that the ground-state center of mass function always is $\Upsilon_0(\vec{R}) = CN^{3/4} \exp[-NR^2/(2b_t^2)]$. Then equation (15) is a product of the lowest solution for the motion of the center of mass in a trap, and the lowest hyperspherical wave function $F_0\Phi_0$ in equation (9), where $F_0(\rho) \propto \exp[-\rho^2/(2b_t^2)]$ and the angular part $\Phi_0(\rho, \Omega)$ is a constant. This relation in equation (15) between ordinary cartesian and hyperspherical coordinates is valid for any length parameter b_t . Therefore a product of identical single-particle Gaussian wave functions is equivalent to a hyperradial Gaussian and a constant angular wave function. This implies equivalence between mean-field Gaussian wave functions and lack of dependence on hyperangles Ω .

In reality the interactions produce (weaker or stronger) correlations and the hyperspherical wave function deviates from a hyperradial Gaussian multiplied by a constant hyperangular part. Therefore the mean-field Hartree product wave function is strictly not exact. However, a measure can be obtained by calculating the single-particle density

$$n(\vec{r}_1) = \int d^3\vec{r}_2 d^3\vec{r}_3 \cdots d^3\vec{r}_N |\Psi(\rho, \Omega) \Upsilon(\vec{R})|^2, \quad (16)$$

which can be compared with the mean-field analogue $|\psi_{\text{s.p.}}(\vec{r}_1)|^2$. The $3(N-1)$ -dimensional integral in equation (16) is very complicated with the full numerical hyperspherical solution. To get an idea of the possible structures we assume a constant angular part $\Phi(\rho, \Omega)$. We expand the hyperradial density distribution on Gaussian amplitudes with different length parameters a_j :

$$|F(\rho)|^2 = \sum_j c_j \frac{2}{\Gamma(\frac{3N-3}{2}) a_j^{3N-3}} e^{-\rho^2/a_j^2}, \quad (17)$$

where $\sum_j c_j = 1$ assures that $F(\rho)$ is normalized as $\int_0^\infty d\rho \rho^{3N-4} |F(\rho)|^2 = 1$. This yields

$$n(\vec{r}_1) = \sum_j c_j \frac{1}{\pi^{3/2} B_j^3} e^{-r_1^2/B_j^2}, \quad B_j^2 = \frac{(N-1)a_j^2 + b_t^2}{N}, \quad (18)$$

which is equivalent to $\langle r_1^2 \rangle = \int d^3\vec{r}_1 n(\vec{r}_1) r_1^2$, since

$$\langle r_i^2 \rangle = \frac{1}{N} \langle \rho^2 \rangle + \langle R^2 \rangle = \frac{3}{2} \left(1 - \frac{1}{N}\right) \sum_j c_j a_j^2 + \frac{3}{2} \frac{1}{N} b_t^2 \quad (19)$$

and

$$\begin{aligned} \int d^3\vec{r}_1 n(\vec{r}_1) r_1^2 &= \frac{3}{2} \sum_j c_j B_j^2 \\ &= \frac{3}{2} \left(1 - \frac{1}{N}\right) \sum_j c_j a_j^2 + \frac{3}{2} \frac{1}{N} b_t^2 \sum_j c_j = \langle r_i^2 \rangle. \end{aligned} \quad (20)$$

The mean square distance between the particles can then be obtained from the Gross-Pitaevskii, or mean-field, approximation for $\langle r_i^2 \rangle$ by the relation

$$\langle r_{ij}^2 \rangle = \frac{2N}{N-1} \left(\langle r_i^2 \rangle - \langle R^2 \rangle \right) = \frac{2N}{N-1} \left(\langle r_i^2 \rangle - \frac{1}{N} \frac{3}{2} b_t^2 \right). \quad (21)$$

For a non-interacting gas in a harmonic external field the energy E_0 is related to $E_0 \propto \langle r_i^2 \rangle$ by the virial theorem.

These relations are derived and valid only for Gaussian wave functions. However, the true mean-field solution is not strictly a Gaussian, although such an approximation is rather efficient as pointed out by Pethick *et al.* [4]. The above results can be used to relate an approximate Gaussian mean-field density distribution to a similar hyperradial distribution implicitly, assuming constant angular wave function corresponding to uncorrelated structure, see Bohn *et al.* [14].

2.2.2. Faddeev-Yakubovskii description. We seek the effect of correlations and have to operate beyond the mean-field. Let us first consider the Faddeev-Yakubovskii techniques where the proper asymptotic behaviour of the wave functions directly is taken into account [21, 22]. This formulation is well suited when the large distance asymptotics crucial as expected for low-density systems.

Faddeev initially studied three-particle systems ($N = 3$) where one of the two-body subsystems was bound, and the other subsystems were unbound [21]. He wrote the wave function as $\Psi = \Phi_{12} + \Phi_{13} + \Phi_{23}$ with the three terms given by suitable permutations of

$$\Phi_{23} = \phi_{23}(\vec{r}_{23}) e^{i\vec{k}_1 \vec{r}_1 + i\vec{K}_{23} \vec{R}_{23}}, \quad (22)$$

where $\vec{R}_{23} = (m_2 \vec{r}_2 + m_3 \vec{r}_3) / (m_2 + m_3)$ is the center of mass of the bound subsystem and \vec{K}_{23} is the conjugate wave vector. A generalization of this three-body wave function is

$$\Phi_{ij} = \phi_{ij}(\vec{r}_{ij}) \exp \left(i \sum_{k \neq i,j} \vec{k}_k \vec{r}_k + i \vec{K}_{ij} \vec{R}_{ij} \right), \quad \Phi = \sum_{i < j}^N \Phi_{ij}. \quad (23)$$

When all relative energies are small, $K_{ij} \simeq 0$ and $k_k \simeq 0$, we obtain $\Phi_{ij} \simeq \phi_{ij}(\vec{r}_{ij})$.

Generalization to an N -particle system was formulated by Yakubovskii who arranged the particles into all possible groups of subsystems and thereby formally was able to include the correct large-distance asymptotic behaviour for all cluster divisions [22]. The decisive physical properties are related to the division into clusters which for $N = 3$ amounts to three possibilities. The three Faddeev components are related to the number of divisions and not the number of particles. For $N > 3$ the number of cluster divisions is much larger than N . For N particles the wave function is therefore written as a sum over possible clusters

$$\Phi = \sum_{\text{clusters}} \phi(\text{cluster}). \quad (24)$$

This method is often applied with success in nuclear physics [23, 24, 25]. In a dilute system two close-lying particles are found much more frequently than any other cluster configuration. Then the dominating terms in the general cluster expression in equation (24) are the two-body clusters where the remaining particles can be considered uncorrelated and described by plane waves or in the mean-field approximation. The wave function then reduces to the form

$$\Phi(\rho, \Omega) = \sum_{i < j}^N \phi_{ij}(\rho, \Omega). \quad (25)$$

2.2.3. Jastrow procedure. The Jastrow variational formulation was designed to account for correlations [26, 27, 28]. We will briefly comment on the Jastrow ansatz, since it provides a physically transparent reason for writing the wave function as a Faddeev sum in the dilute limit. A connection between the Jastrow ansatz for the relative wave function [28]

$$\Psi(\rho, \Omega) = \prod_{i < j}^N \psi(\vec{r}_{ij}) \quad (26)$$

and the Faddeev formulation is possible. We write the two-body Jastrow component as a mean-field term multiplied by a modification expected to be important only at small separation, i.e., (omitting normalization)

$$\psi(\vec{r}_{ij}) = e^{-r_{ij}^2/(2Nb_t^2)} [1 + \phi(\vec{r}_{ij})], \quad \phi(\vec{r}) = 0 \quad \text{for } r > r_0, \quad (27)$$

where we introduced the length scale r_0 beyond which deviations due to correlations vanish. With equation (3) this leads to the relative wave function

$$\Psi(\rho, \Omega) = e^{-\rho^2/(2b_t^2)} \prod_{i < j}^N [1 + \phi(\vec{r}_{ij})] \quad (28)$$

$$= e^{-\rho^2/(2b_t^2)} \left[1 + \sum_{i < j}^N \phi(\vec{r}_{ij}) + \sum_{i < j \neq k < l}^N \phi(\vec{r}_{ij})\phi(\vec{r}_{kl}) + \dots \right], \quad (29)$$

where we now through equation (15) can see that the Gaussian mean-field Hartree-ansatz is obtained for a non-interacting system in the harmonic external field. For a homogeneous density distribution with $b_t \rightarrow \infty$ the mean-field solution is simply a constant [29]. For a sufficiently dilute system it is unlikely that more than two particles simultaneously are close in space, i.e., both $r_{ij} < r_0$ and $r_{kl} < r_0$. Therefore the expansion in equation (29) can be truncated after the first two terms, i.e.,

$$\prod_{i < j}^N [1 + \phi(\vec{r}_{ij})] \simeq 1 + \sum_{i < j}^N \phi(\vec{r}_{ij}) = \sum_{i < j}^N \left[\frac{1}{N(N-1)/2} + \phi(\vec{r}_{ij}) \right]. \quad (30)$$

Redefining the two-body amplitude we end up with a Faddeev-like sum as in equation (25).

2.3. Two-body s-wave correlations

The conclusion from the preceding two subsections is that a relative wave function of the form

$$\Psi(\rho, \Omega) = F(\rho) \sum_{i < j}^N \phi(\rho, r_{ij}) \quad (31)$$

incorporates both the mean-field properties through $F(\rho)$ and the correlations in addition to the mean-field through the Faddeev-components ϕ . We therefore decompose

the angular wave function Φ in equation (9) (omitting indices ν), into the symmetric expression of Faddeev components ϕ

$$\Phi(\rho, \Omega) = \sum_{i < j}^N \phi_{ij}(\rho, \Omega) \approx \sum_{i < j}^N \phi(\rho, r_{ij}), \quad (32)$$

where the last approximation assumes that only relative s -waves contribute, leaving the dependence on the distance $r_{ij} = \sqrt{2\rho} \sin \alpha_{ij}$. This form emphasizes two-body correlations while excluding explicit multi-body clusterizations. We have “only” assumed relative s -waves between each pair of particles as appropriate for small relative energies and large distances. The capability of this decomposition for large scattering length has been demonstrated for $N = 3$ by an application to the intricate Efimov effect, which also arises precisely for small energies and large distances [30, 31].

The Faddeev ansatz in equation (25) can be formally established as a generalized partial wave expansion in terms of the hyperspherical harmonic kinetic energy eigenfunctions. The two-body s -wave simplification then appears as a truncation of this expansion to include only the lowest hyperharmonics for the description of the remaining $N - 2$ particles. Since this function is a constant we arrive at equation (32).

In conclusion, we believe that the Faddeev ansatz with two-body amplitudes accounts for the important two-body correlations when the system is sufficiently dilute, and at the same time keeps the mean-field information about motion relative to the remaining particles. An extension of this technique would be a feasible, but perhaps intricate, approach to study three-body correlations in denser systems and in connection with the important process of three-body recombination within N -body systems.

3. General properties

The method outlined above leads to the effective radial potential in equation (12) and the radial equation (11). This huge simplification is hiding all the complications and the detailed information in the angular eigenvalue computations. The key quantity is then the function λ , which determines the properties of the radial potential.

The angular eigenvalue equation (10) can by a variational technique be rewritten as a second-order integro-differential equation in the variable α_{12} [19]. For atomic condensates the interaction range is very short compared with the spatial extension of the N -body system. Using this short-range property of the interaction in the integro-differential equation simplifies even further to contain at most one-dimensional integrals. The validity of our approximations only relies on the small range of the potential, whereas the scattering length can be as large as desired.

We shall apply a Gaussian potential $V(r) = V_0 \exp(-r^2/b^2)$ and study dependence on the scattering length a_s for a fixed range b . It is convenient to measure the strength of the interaction in units of the Born-approximation a_B of the scattering length

$$a_B \equiv \frac{m}{4\pi\hbar^2} \int d^3\vec{r}_{kl} V(\vec{r}_{kl}), \quad (33)$$

which for the Gaussian potential is $a_B = \sqrt{\pi}mb^3V_0/(4\hbar^2)$.

3.1. Angular potential

The effective two-body interactions can vary enormously for different systems and different experiments. The general structure for neutral atoms is an attraction at longer distances arising from mutually induced polarization. At shorter distances the Pauli blocking dominates and causes the effective interaction to be repulsive. Depending on the strength of the interaction the two particles may form a bound state of relatively small radius (nm) compared to the typical size (μm) of a Bose-Einstein condensate. For the alkali atoms there are usually several of such bound two-body states.

Scattering of two atoms at sufficiently low relative energy depends only on the two-body s -wave scattering length a_s . Large distances appropriate for dilute systems can then be expected to be determined almost entirely by a_s . At higher densities also the effective range of the interaction may be significant.

We expect that two-body interactions are responsible for the properties of the many-body system. In our formulation, first the properties of the angular eigenvalues are determined and next they enter decisively the effective potentials and the radial equations. Qualitatively the results depend on the sign of the scattering length and the number of two-body bound states. This is understandable as the atoms in a dilute system at low energy effectively interact as in a two-body scattering situation. Higher-order processes seldom occur and do not contribute to the properties of the dilute system.

The study in [17] included variations of the interaction strength and the number of particles. We show in figure 1 the lowest angular potential for $N = 100$ for Gaussian two-body interactions with various scattering lengths. When $a_s = -b$ (solid line) the potential has no bound two-body states. The lowest angular eigenvalue is zero at $\rho = 0$, decreases then through a minimum as a function of ρ and continues afterwards to approach zero at large hyperradii as a_s/ρ . Increasing the attraction (broken lines) decreases all angular eigenvalues for all ρ -values. The details at smaller hyperradii hardly change with large variations of the scattering length. However, at larger distances the approach towards zero is converted into a parabolic divergence as soon as the scattering length jumps from negative (dotted) to positive (dot-dashed) corresponding to the appearance of a bound two-body state.

Generally, an attractive finite-range interaction can support a certain number N_B of two-body bound states for both positive and negative scattering lengths. Then the lowest angular eigenvalues, $\lambda_0, \lambda_1, \dots, \lambda_{N_B-1}$, describe these bound two-body states within the many-body system at large hyperradii, i.e., they diverge to $-\infty$ as seen in figure 1. The next eigenvalue λ_{N_B} converges to zero at large distance and corresponds to the first “two-body-unbound” mode. Through the derived adiabatic potential this mode is responsible for the properties of atomic Bose-Einstein condensation, where no clusterization is allowed.

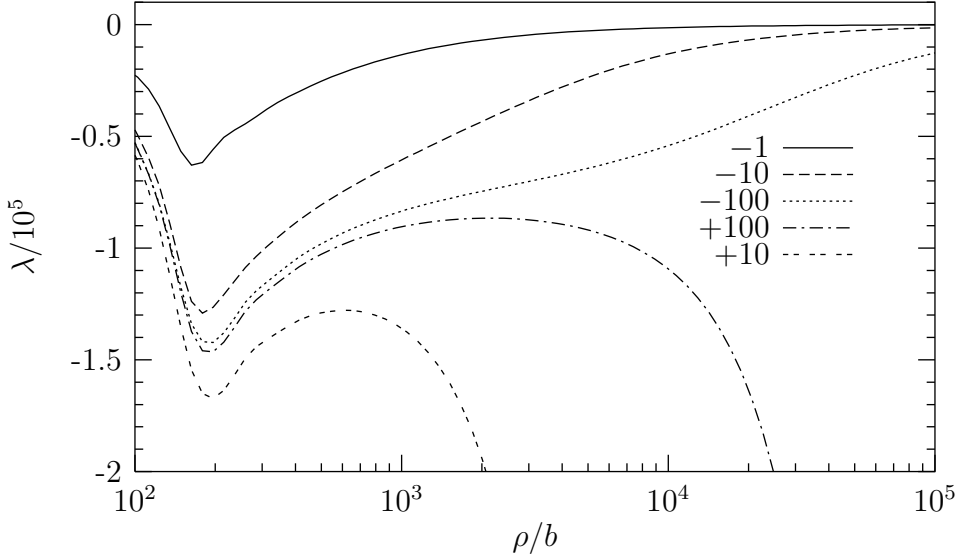


Figure 1. The lowest angular eigenvalues λ for $N = 100$ bosons interacting via a Gaussian two-body potential $V(r) = V_0 \exp(-r^2/b^2)$ with zero or one bound two-body states. The scattering lengths a_s/b are indicated on the figure.

The detailed numerical analysis in [17] resulted in a simple parametrization for the behaviour of these λ -functions. Let us here restrict ourselves to attractive two-body interactions in two different regimes: i) no bound two-body states and $a_s < 0$, and ii) one bound two-body state and $a_s > 0$. For hyperradii exceeding a lower limit ρ_0 , which roughly is at the minimum, i.e., $\rho > \rho_0 \equiv 0.87N^{1/2}(b/|a_s|)^{1/3}b$ the analytical expressions are [17]

$$\begin{aligned} \lambda_a(N, \rho) = & -|\lambda_\delta(N, \rho)| \left(1 + \frac{0.92N^{7/6}b}{\rho} \right) \\ & \times \begin{cases} 1 - \exp \left(-\frac{|\lambda_\infty(N)|}{|\lambda_\delta(N, \rho)|} \right) & \text{when } a_s < 0, \\ \frac{|\lambda_\infty(N)|}{|\lambda_\delta(N, \rho)|} + \frac{|\lambda^{(2)}(\rho)|}{|\lambda_\delta(N, \rho)|} & \text{when } a_s > 0, \end{cases} \end{aligned} \quad (34)$$

where λ_δ is the expectation value of \hat{h}_Ω for the zero-range interaction $V_\delta(\vec{r}) = 4\pi\hbar^2 a_s \delta(\vec{r})/m$ in a constant angular wave function $\Phi(\rho, \Omega) = \text{constant}$, i.e.,

$$\lambda_\delta(N, \rho) = \sqrt{\frac{2}{\pi}} \frac{\Gamma(\frac{3N-3}{2})}{\Gamma(\frac{3N-6}{2})} N(N-1) \frac{a_s}{\rho} \xrightarrow{N \gg 1} \frac{3}{2} \sqrt{\frac{3}{\pi}} N^{7/2} \frac{a_s}{\rho}, \quad (35)$$

$$\lambda_\infty(N) = -1.59N^{7/3}, \quad (36)$$

$$\lambda^{(2)}(\rho) = E^{(2)} \frac{2m\rho^2}{\hbar^2}, \quad E^{(2)} = -\frac{\hbar^2}{m|a_s|^2} c. \quad (37)$$

The number c approaches unity when the scattering length becomes very large. The factor $(1 + 0.92N^{7/6}b/\rho)$ reflects dependence on potential details like the finite range b of the Gaussian two-body interaction. At $\rho \sim N^{7/6}|a_s|$ we have $\lambda_\delta \sim \lambda_\infty \sim \lambda^{(2)}$. For small hyperradii $\rho < \rho_0$ we use for all a_s the perturbation result obtained as the expectation

value of the two-body interaction in a constant angular wave function, i.e.,

$$\lambda_a = \lambda^{(0)}(\rho) \equiv \frac{mV(0)N^2\rho^2}{\hbar^2}, \quad \text{for } \rho < \rho_0, \quad (38)$$

where we use equation (38) for small ρ when $|\lambda^{(0)}(\rho)|$ is smaller than the expression equation (34). Then the angular eigenvalue λ is defined analytically for all ρ . These expressions describe rather accurately the results of full numerical computations for any two-body interaction as soon as ρ is larger than ρ_0 . We should emphasize that the small-distance region where $\lambda_a = \lambda^{(0)}(\rho)$ is sensitive to the specific choice of two-body interaction.

The results of the parametrization in equations (34) and (38) are illustrated in figure 2 for $N = 100$ for various scattering lengths. The pronounced deep minimum

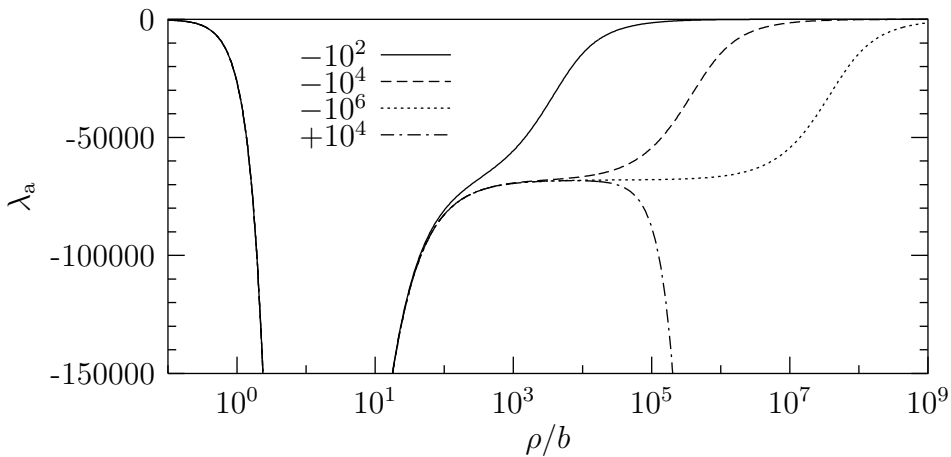


Figure 2. The angular eigenvalue λ , equations (34) and (38), for $N = 100$ as function of ρ for the different scattering lengths given on the figure in units of the range a_s/b .

at $\rho \sim \rho_0$ is in the region depending on the two-body potential and reflects only the qualitative behaviour of the numerically correct lowest angular eigenvalue. After this strongly attractive region at small ρ the eigenvalues approach zero. As the size of the scattering length increases the eigenvalue develops a plateau at a constant value λ_∞ independent of a_s . Eventually at large ρ the eigenvalues vanish as λ_δ for $a_s < 0$ and diverges to $-\infty$ when $a_s > 0$.

When $a_s < 0$ the analytic and the correct eigenvalues both exceed the asymptotic zero-range result, i.e., $\lambda_a \geq \lambda_\delta$ for all hyperradii. This means that the true ground state energy is higher than the energy obtained with the zero-range interaction. Thus the ground state energy from our model is higher than the mean-field energy. The origin of this sequence of energies is that the zero-range interaction inevitably leads to diverging energies for smaller distances. The present model avoids this non-physical short-range collapse.

When $a_s > 0$ the interaction is effectively repulsive at large hyperradii and we find analogously that an analytical expression in this case for the second angular eigenvalue obeys $\lambda_a \leq \lambda_\delta$ for all hyperradii, due to the divergence of $\lambda_\delta \rightarrow +\infty$ as $\rho \rightarrow 0$.

Correspondingly we get energies smaller than the zero-range mean-field result in the positive a_s -case. Bohn *et al.* [14] obtained in this case only energies higher than the Gross-Pitaevskii energy.

3.2. Radial potential

The parametrization in equation (34) leads to an analytic expression for the radial potential. We can then also study the properties of the radial potential and derive physical quantities like the energy and the root-mean-square separation between bosons. In particular the attractive two-body potentials generally give rise to a large number of negative-energy many-body states. Using the method described in [32] it is possible to estimate the number \mathcal{N} of such bound states, i.e.,

$$\mathcal{N} \simeq \frac{\sqrt{2m}}{\pi\hbar} \int \sqrt{|U^{(-)}(\rho)|} d\rho, \quad (39)$$

where $U^{(-)(\rho)}$ denote the negative part of the radial potential $U(\rho)$.

3.2.1. Features of the analytic expression. The radial potential obtained from equation (34) is shown in figure 3 as function of the hyperradius for a series of different particle numbers and scattering lengths. The strongly varying short-distance dependence is omitted to allow focus on intermediate and large hyperradii. When an intermediate barrier is present the condensate is described as the state of lowest energy located in the minimum at large hyperradius. This minimum exists for $a_s < 0$ when $N|a_s|/b_t < 0.5$ as established in [14, 16]

The behaviour at very small hyperradii can be constructed from equation (38). However, now the central value of the two-body interaction enters explicitly and the resulting radial potential therefore depends on the short-distance behaviour of this interaction. This model-dependence extends to larger distances where the perturbation expression in equation (38) is invalid. This region of ρ up to \sqrt{Nb} is not very interesting in the present context and we therefore only crudely connected the analytic parametrization in equation (34) and the expression in equation (38) to allow extraction of the model-independent result.

Moving alphabetically in figure 3 from (a)-(f) we first in (a)-(d) maintain the particle number $N = 6000$ while only the scattering length a_s varies. From (d)-(f) we maintain $a_s/b = -0.35$ and vary N . In (a) the two-body interaction is zero, $a_s = 0$, leading to a vanishing angular eigenvalue, $\lambda = 0$. The effective radial potential then consists only of centrifugal barrier and external field with one minimum. In (b) we turn on an attractive potential, $a_s = -0.05b$, sufficiently strong to overcompensate for the centrifugal repulsion and create a second minimum in the radial potential at smaller hyperradius. An intermediate barrier is left between the two minima at small and large hyperradii. A further increase of the attraction in (c) removes the barrier while leaving a smaller, flat region. The negative-potential region around the minimum at small

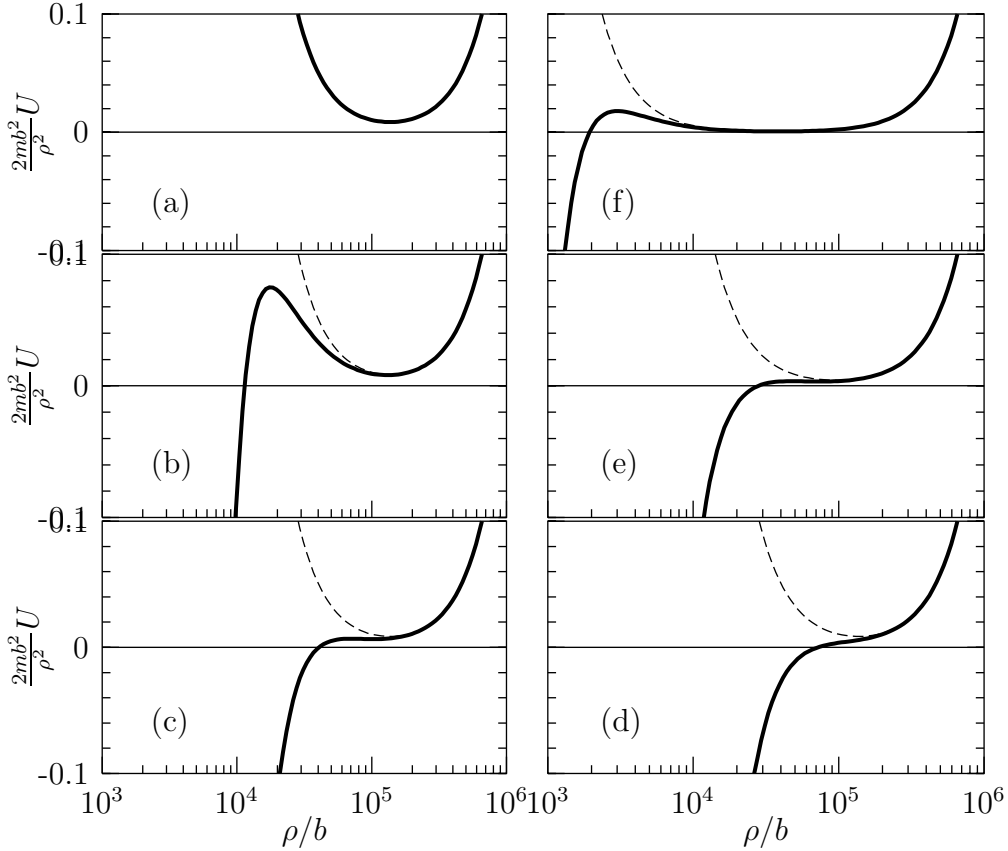


Figure 3. Radial potentials with $b_t/b = 1442$ and (a) $N = 6000$, $a_s \sim 0$; (b) $N = 6000$, $a_s/b = -0.05$; (c) $N = 6000$, $a_s/b = -0.18$; (d) $N = 6000$, $a_s/b = -0.35$; (e) $N = 3000$, $a_s/b = -0.35$; (f) $N = 500$, $a_s/b = -0.35$. The dashed lines are with $a_s = 0$. The divergence $U(\rho) \rightarrow +\infty$ when $\rho \rightarrow 0$ is not shown.

hyperradius is now even more pronounced. This tendency is continued in (d) with a stronger attraction.

With the scattering length from (d), $a_s = -0.35b$, and a decreasing number of particles the intermediate barrier is slowly restored while moving to smaller hyperradii. In (e) for $N = 3000$ a barrier is about to occur, and in (f) with only $N = 500$ an intermediate barrier is again present between a minimum at small and large hyperradii.

3.2.2. Large scattering length A large scattering length implies through equation (34) an intermediate region in hyperradius where the angular potential is almost constant. More specifically, when $\rho < N^{7/6}|a_s|$ and $\lambda \simeq \lambda_\infty$ two of the terms in the radial equation (12) add to a negative value

$$\frac{\lambda_\infty}{\rho^2} + \frac{(3N-4)(3N-6)}{4\rho^2} < 0, \quad (40)$$

which implies that no repulsive barrier is present. Then the effective potential is ρ^{-2} until the trap begins to dominate.

We show in figure 4 the analytic radial potential corresponding to one of the angular

eigenvalues from figure 2. We observe that the radial potential is negative in a large range of hyperradii which can be divided into three different regions. For small hyperradii the radial potential has a minimum. For intermediate hyperradii the angular potential is a constant and therefore the radial potential behaves as $-1/\rho^2$. This is from figure 2 seen to appear for ρ/b between 10^2 and 10^5 . When $\rho \geq N^{7/6}|a_s|$ the angular potential vanishes as $-1/\rho$, so the radial potential vanishes as $-1/\rho^3$, although not clear on the figure. Finally the trap $\propto \rho^2$ dominates with positive contributions at large hyperradii.

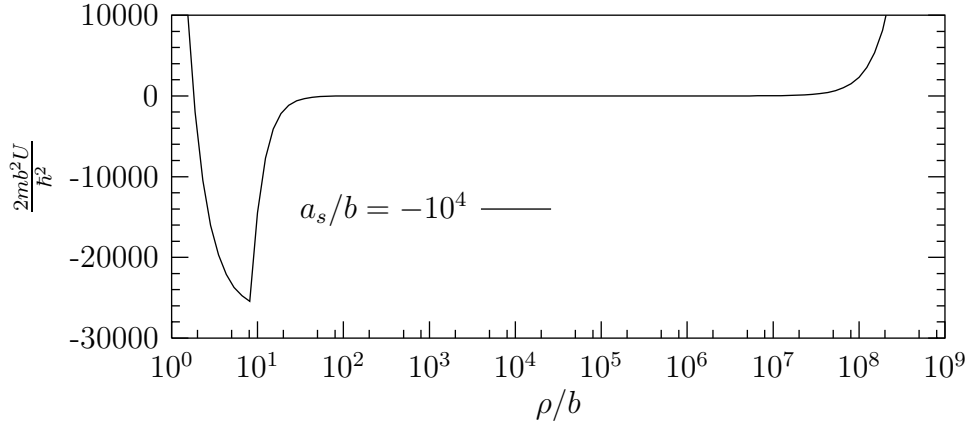


Figure 4. Analytic radial potential obtained from equations (12) and (34) for $N = 100$ and $a_s/b = -10^4$.

The bound states in this potential can be divided into groups according to their hyperradial extension. The total number of such states is written as $\mathcal{N} = \mathcal{N}_1 + \mathcal{N}_E + \mathcal{N}_2$ where \mathcal{N}_1 , \mathcal{N}_E , and \mathcal{N}_2 are the number of states located respectively in the attractive pocket at small hyperradii, in the intermediate $-1/\rho^2$ region and at hyperradii large compared with the scattering length.

With the analytic expressions inserted into equation (39) to obtain the effective potential we find a crude estimate of the number of self-bound states in the pocket to be $\mathcal{N}_1 \simeq 1.3N^{3/2}$. This number depends on the properties of the two-body potential but the $N^{3/2}$ scaling remains unchanged for all short-range interactions. The outer region also supports bound states when the trap length b_t is sufficiently large, i.e., $b_t \gg N|a_s|$, where we analogously find that $\mathcal{N}_2 \simeq 0.78N^{7/6}$. This number may be severely influenced by the confinement of the external trap, but again the $N^{7/6}$ scaling remains unchanged.

The intermediate region is only present when the scattering length is relatively large. This region exist when

$$b \ll \frac{\rho}{N^{7/6}} \ll |a_s| , \quad (41)$$

where these limits correspond to values of the hyperradius larger than $\rho_{\min} = N^{7/6}b$ and smaller than $\rho_{\max} = N^{7/6}|a_s|$. The number of Efimov-like states \mathcal{N}_E located in this region is then given by equation (39), see [33, 15]. This gives

$$\mathcal{N}_E \simeq \frac{|\xi|}{\pi} \ln \left(\frac{\rho_{\max}}{\rho_{\min}} \right) , \quad (42)$$

$$\xi^2 \equiv -\lambda_\infty - \frac{(3N-4)(3N-6)}{4} - \frac{1}{4} \approx 1.59N^{7/3}, \quad (43)$$

where we used equation (36) and assume N is large. The number of these bound states is then

$$\mathcal{N}_E \simeq 0.40N^{7/6} \ln \left(\frac{|a_s|}{b} \right). \quad (44)$$

This estimate assumed that the external trap has no influence on the hyperradial potential for $\rho < \rho_{\max}$. However, when the trap length b_t is sufficiently small, i.e., when $\rho_{\text{trap}} = \sqrt{Nb_t} < N^{7/6}|a_s|$, the extension of the plateau is truncated at large hyperradii. The number of states can then be estimated by substituting ρ_{\max} with ρ_{trap} in equation (42). This yields

$$\mathcal{N}_E \simeq 0.40N^{7/6} \ln \left(\frac{\sqrt{3/2}b_t}{N^{2/3}b} \right). \quad (45)$$

The plateau can not exist when the external potential dominates already at small distances, i.e., for short trap lengths when $\rho_{\text{trap}} < N^{7/6}b$ or equivalently $N \gtrsim N_{\max} \equiv (b_t/b)^{3/2}$. This maximum number of particles allowing a plateau and the resulting Efimov-like states is for a realistic ratio of $b_t/b = 1442$ therefore obtained to be $N_{\max} \simeq 55000$. This estimate is rather uncertain but it illustrates that too many particles not only exclude stability of the condensate but also the existence of the spatially extended Efimov-like structures which otherwise might play a role in the recombination processes.

The number of Efimov-like states \mathcal{N}_E increases strongly with N as seen in table 1 for $b_t/b = 1442$ for a few particle numbers. These estimates are more precise than in previous work where we obtained $\mathcal{N}_E = 28$ for $N = 20$ for the same parameters [15].

N	10	20	100	1000	10000
\mathcal{N}_E	35	72	380	3632	24810

Table 1. The number \mathcal{N}_E of Efimov-like states for $b_t/b = 1442$ and $|a_s| \rightarrow \infty$.

The energies and mean square radii of the Efimov-like states are related by the expressions [33]

$$E_n = -\frac{\hbar^2}{2m\langle \rho^2 \rangle_n} \frac{2}{3}(1 + \xi^2), \quad E_n = E_0 e^{-2\pi n/\xi}, \quad (46)$$

where the exponential dependence on both the strength ξ of the effective potential and the number of excited states is highlighted.

Let us assume that the trap length is large and not responsible for terminating the plateau at large distance. We can then crudely assume that the mean square hyperradius of the first and last Efimov-like states are given by $\rho_{\min}^2 = N^{7/3}b^2$ and $\rho_{\max}^2 = N^{7/3}|a_s|^2$, respectively. Using equation (46) we then obtain the energies of the first and last Efimov-like states

$$E_{\text{first}} \simeq -\frac{\hbar^2}{2mb^2}, \quad E_{\text{last}} \simeq -\frac{\hbar^2}{2m|a_s|^2}. \quad (47)$$

which turn out to be independent of the particle number N . Furthermore, these energies look familiar as the kinetic energy scale of strongly bound two-body states and the expression for a weakly bound or a resonance two-body energy, respectively. This does not mean that the average distance \bar{r} between two particles in these many-body states also are given by b and a_s . In fact, \bar{r} contains an additional N -dependent factor, i.e., $\bar{r} \approx N^{2/3}b, N^{2/3}|a_s|$ for the two cases.

These constant energy limits obviously imply that the density of Efimov-like states increases with particle number precisely as the interval scales, i.e., $N^{7/6}$.

3.2.3. Decay and collapse. The Bose-Einstein condensate is intrinsically unstable and decays spontaneously. In addition changes of the decisive parameters after creation of a specific structure could lead to immediate instability and much faster decays better described as a collapse. In the experiments by Donley et al. [7] a condensate was first created with effectively zero interaction, i.e., zero scattering length as in figure 3a. The radial wave function is then located at relatively large distances in the minimum created by the compromise between centrifugal barrier and external field. The attractive pocket at small distances is not present and the condensate appears as the ground state in this potential. Both the radial potential and the wave function are shown in figure 5.

In the experiment the effective interaction was then suddenly changed by tuning a Feshbach resonance [34] to obtain a large and negative scattering length [7]. The corresponding radial potential, also shown in figure 5, has a pronounced attractive region able to support a number of bound states. After this sudden change of potential the initial wave function is no longer a stationary state in the new potential. Nothing is holding it back from moving to small hyperradii, where it would be reflected from the centrifugal barrier wall, if all particles remain in the condensate. The time dependent wave function corresponds to an oscillation between the walls of the centrifugal barrier and the external field.

Expansion on the eigenfunctions in the new potential then produces a specific time dependence of given periodicity. The dominating states in this expansion are the highest-lying Efimov-like states now present because of the large scattering length which produces the plateau region and the ρ^{-2} potential. These states are as spatially extended as the initial wave function. The mean square hyperradius and the average distance between pairs of particles are both smallest after a quarter of a period of the oscillation. The wave function at this time T is also shown in figure 5.

It should be emphasized that the sudden change of potential and the subsequent motion towards small hyperradii is a dynamical process which most likely also involves the angular degrees of freedom. The expansion on the lowest adiabatic potential is therefore not necessarily very accurate, but perhaps providing a lower limit of the time before decay by recombination. Exploiting other higher-lying adiabatic potentials would slow down the radial motion and the times would be longer.

The decay probability increases enormously with decreasing hyperradius simply due to the higher density which forces several particles to be close in space and therefore

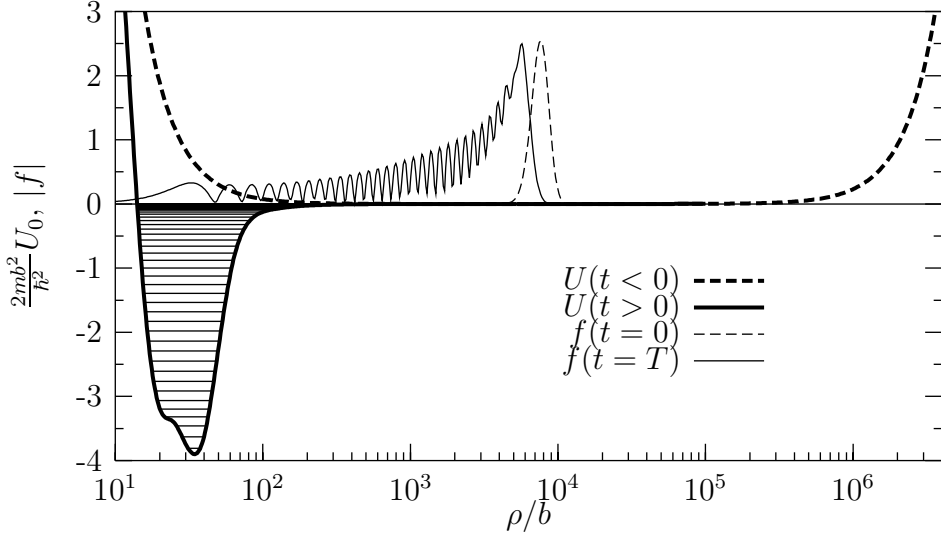


Figure 5. Wave functions f and effective hyperradial potentials U in dimensionless units as function of hyperradius for $N = 20$. The scattering length is zero up to the time $t = 0$ and then suddenly changes to be large and negative at later times $t > 0$. Potentials and the corresponding wave functions are sketched for $t = 0$ and at a time T after a quarter of a period. The horizontal lines show the stationary negative-energy states for $t > 0$.

much more likely to recombine into molecular states. The dominating process is expected to be three-body recombination producing two-body bound states. The time scale for this decay is given by $N(t) = N(0) \exp(-t/T_{\text{rec}})$, where N is the number of atoms in the condensate. This is as a function of the average hyperradius $\bar{\rho}$ estimated by [17]

$$T_{\text{rec}} = \frac{2m\bar{\rho}^6}{\hbar|a_s|^4 N^3}. \quad (48)$$

This recombination time for the highest-lying Efimov-like states ($\bar{\rho} \approx N^{7/3}|a_s|$) can then be compared to the time scale for motion in the condensate which is given by $T_{\text{trap}} \approx 2\pi/\omega$. We find

$$\frac{T_{\text{rec}}}{T_{\text{trap}}} \approx \frac{N^2}{\pi} \left(\frac{N|a_s|}{b_t} \right)^2. \quad (49)$$

Thus, close to the limit of stability established as $N|a_s|/b_t \sim 0.5$, we have $T_{\text{rec}} \gg T_{\text{trap}}$ ($N \gg 1$) and the recombination process is rather slow for these highest-lying Efimov-like states. Still the lifetime must in all cases be much shorter than for the initially created condensate simply because the density is larger.

If these Efimov-like states are populated in experiments where the potential suddenly is changed from figure 3a to figure 3c,d,e, they could possibly be indirectly observed. A signature of this many-body Efimov effect would be observation of the diatomic molecules formed in the recombination process and with the estimated rate T_{rec} derived from equation (49). The rate should then be inversely proportional to the square of the scattering length reached after changing the potential.

These Efimov-like states may exist as quasistationary states sufficiently decoupled

from all the other many-body degrees of freedom to be observed in experiments. The recombination time or rather the corresponding width $\Gamma_{\text{Efimov}} = \hbar/T_{\text{rec}}$ of the Efimov-like states indicates the degree of decoupling. Using equations (46) and (47) we obtain

$$\frac{\Gamma_{\text{Efimov}}}{E_n - E_{n-1}} \approx \frac{1}{4\pi^2 N^{11/6}} \left(\frac{b}{a_s} \right)^2, \quad \frac{\Gamma_{\text{Efimov}}}{E_n - E_{n-1}} \approx \frac{1}{4\pi^2 N^{11/6}} \quad (50)$$

for the first and last Efimov-like states, respectively. The couplings compared to the level spacings are small and decreasing with N . Thus the identities of these states could be very well preserved within the many-body system. Still their lifetimes due to recombination processes can be very large compared to the time scale defined by the external field.

4. Connections to the mean-field approximation

The mean-field is often used to describe a condensate. A Hartree product of single-particle wave functions describes very successfully a Bose-Einstein condensate of a dilute, weakly interacting gas of pointlike particles with $n|a_s|^3 \ll 1$ where n is the density. The reason is that the mean-field validity condition is then fulfilled, i.e., the mean free path is long compared to the interaction range of the system defined by the scattering length. The low-energy scattering properties expressed by the scattering length are then clearly decisive. In the following we first comment on the choice of interaction and second on the differences between the mean-field method and the hyperspherical adiabatic method. Finally we discuss the conditions of validity.

4.1. The two-body interaction

The choice of the interactions should be strongly correlated with the Hilbert spaces available for the different methods. In the mean-field treatment a zero-range interaction is often applied

$$V_\delta(\vec{r}) = \frac{4\pi\hbar^2 a_s}{m} \delta(\vec{r}), \quad (51)$$

where a_s is the two-body s -wave scattering length. This limit can be obtained from a finite range potential where the range approaches zero and the strength is appropriately adjusted. We use a finite-range Gaussian interaction

$$V_G(\vec{r}) = V_0 e^{-r^2/b^2}, \quad (52)$$

where the Born-approximation a_B to the scattering length then is a measure of the strength, see equation (33). The Gaussian is in the limit when $b \rightarrow 0$ a representation $\Delta_b(\vec{r})$ of the Dirac δ -function

$$\Delta_b(\vec{r}) \equiv \frac{1}{\pi^{3/2} b^3} e^{-r^2/b^2}, \quad 1 = \int d^3 \vec{r} \Delta_b(\vec{r}). \quad (53)$$

We rewrite equation (52) as

$$V_G(\vec{r}) = \pi^{3/2} b^3 V_0 \Delta_b(\vec{r}) = \frac{4\pi\hbar^2 a_B}{m} \Delta_b(\vec{r}), \quad (54)$$

which has the same form as equation (51), but with a_B instead of a_s . Then for $a_s = a_B$ we have

$$\lim_{b \rightarrow 0} V_G(\vec{r}) = V_\delta(\vec{r}) . \quad (55)$$

However, $a_s = a_B$ is only valid when $|a_B|/b \rightarrow 0$, which is rarely the case.

The zero-range limit of vanishing range b can be reached in several ways, e.g., as in equation (54) with a constant a_B or with a b -dependent adjustment of V_0 to keep a constant a_s . These two limits differ enormously and the optimum choice depends on the purpose and the Hilbert space restricting the wave function. If the low-energy scattering properties are crucial the constant a_s seems to be the unavoidable choice. However, this does not lead to equation (51) but the strength of the interaction should instead approach zero linearly with b .

Thus the scattering length is not correct with the normalization in equation (51). In fact it is not even defined for this interaction. Still, the aim of computing reliable energies in the mean-field approximation can be achieved with this strength for dilute systems [35]. The prize to be payed is that the Hilbert space then must be restricted to the mean-field product wave functions. Any extension to include features outside this restricted space for example two-body cluster structures would be disastrous [36]. In other words the wave functions are very difficult to improve even in perturbation theory.

These conclusions reflect the general requirement that the Hilbert space and the interaction must be consistent, i.e., a restricted space requires a renormalized interaction to produce the correct energy. This means that the strength of the zero-range interaction for low-density systems must be chosen to reproduce the correct scattering length by using the first Born approximation [35].

Maintaining the finite range interaction with the correct scattering length then results in completely different properties of the interaction even when the range approaches zero on any scale defined by the physics of the problem. Thus the mean-field product wave function with a realistic two-body potential would also lead to disastrous results. The cure in mean-field theory for the dilute gases is to adjust the interaction to reproduce the correct behaviour at large distances.

Clearly, the full Hilbert space with the correct interaction must produce correct results. Whether the realistic interaction combined with our choice of the space including two-body correlation amplitudes can reproduce the main features is not *a priori* obvious. However, the investigations summarized in the previous section demonstrate that the energy of the mean-field approximation for dilute systems is reproduced and the correct large-distance behaviour is at least approximately obtained. This asymptotic behaviour is determined by the scattering length which only implicitly is contained in a given combination of range and strength of the Gaussian interaction. This implies that our Hilbert space must account properly for the crucial correlations necessary for an accurate description at large distances.

4.2. Hyperspherical formulation with the zero-range interaction

A reformulation of the mean-field in hyperspherical coordinates was given by Bohn *et al.* [14]. They assumed an angular wave function, where all correlations are neglected, and a zero-range interaction, equation (51), is used precisely as in the mean-field approximation. This results in an angular potential produced by the angular eigenvalue λ_δ in equation (35). With this hyperspherical potential they solve the radial equations.

Roughly speaking, our angular potential arising from the Gaussian interaction is above λ_δ when $a_s < 0$, and below when $a_s > 0$. The “exaggeration” in [14] of the zero-range interaction is a result of including the a_s/ρ -divergence of λ_δ also for small distances. When ρ approaches zero or the scattering length diverges, these and other mean-field methods yield disastrous results.

The mean-field interaction energy can be estimated as the expectation value of the δ -function interaction in equation (51) with a normalized Gaussian Hartree wave function:

$$\psi(\vec{r}) = \frac{1}{\pi^{3/4} b_t^{3/2}} e^{-r_i^2/(2b_t^2)}, \quad (56)$$

$$E_{\text{int}} = \frac{N(N-1)}{2} \int d^3\vec{r} \psi^*(\vec{r}) V_\delta(r) \psi(\vec{r}) = \frac{2N(N-1)\hbar^2 a_s}{\sqrt{\pi} m b_t^3}, \quad (57)$$

where we used b_t as the size parameter for the wave function since the confinement is due to the trap. This wave function is then the lowest harmonic oscillator solution obtained without any two-body interaction.

With hyperspherical coordinates this interaction energy is then related to the angular eigenvalue:

$$E_{\text{int}} = \int_0^\infty d\rho f^*(\rho) \frac{\hbar^2 \lambda_\delta(\rho)}{2m\rho^2} f(\rho), \quad (58)$$

where f is the normalized radial Gaussian function corresponding to the Hartree form

$$f(\rho) = \sqrt{\frac{2}{\Gamma(\frac{3N-3}{2}) b_t^{3N-3}}} \rho^{(3N-4)/2} e^{-\rho^2/(2b_t^2)}. \quad (59)$$

This radial wave function is not the correct solution obtained by using the effective potential corresponding to λ_δ . However, only this Gaussian approximation allows an analytic comparison between the hyperspherical and cartesian mean-field wave functions.

4.3. Properties of the wave functions

The Hartree wave function is closely related to the hyperradial function in the dilute limit and the Jastrow correlated wave function is closely related to the Faddeev-like decomposition of the wave function. A direct comparison of the wave functions is not possible in general as this requires an expansion on a complete set of basis functions in one of the coordinate systems. The necessary calculations involve non-reducible $3N$ -dimensional integrals.

Instead we use the indirect relations provided in section 2.2.1, where energy and average distance between particles are characteristic features of the wave function. For a given scattering length the energy E is numerically obtained for a Bose-Einstein condensate as a function of the particle number. We then calculate the interaction energy defined as $E - E_0$ where $E_0 = 3N\hbar\omega/2$ is the energy of the non-interacting, trapped gas. The results are shown in figure 6. For attractive potentials the mean-field has a local minimum at large average distance and much lower (diverging for zero-range) potential energies at small average distances. The mean-field (quasistable) solution is located in the minimum at large average distance. This minimum becomes unstable for sufficiently large particle numbers. In the example of figure 6a no stable mean-field solution exists for $N = 1000$. This is consistent with the stability criterion of about $N|a_s|/b_t < 0.5$ as seen from the x -axis exhibited at the top of the figure.

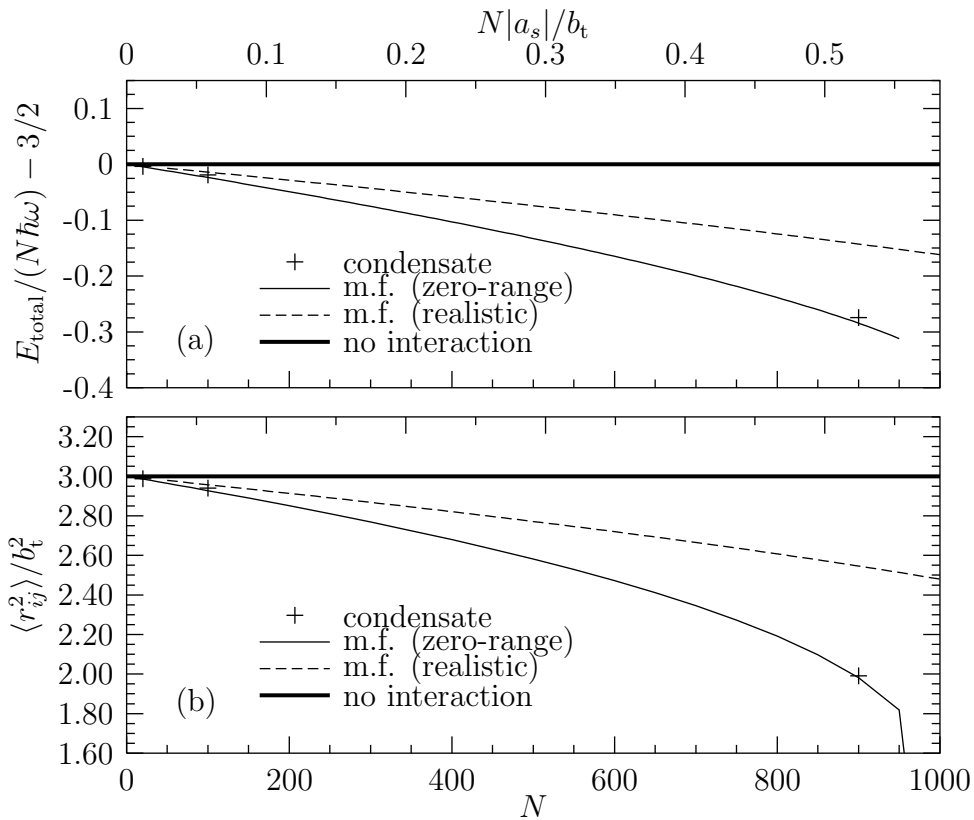


Figure 6. a) Gross-Pitaevskii energy as a function of N for $a_s/b = -0.84$ and $b_t/b = 1442$. Also shown are the hyperspherical calculation for three particle numbers and $a_s/b = -0.84$ ($a_B/b = -0.5$) with quantum numbers as indicated [$n_c = 7$ for $N = 20$ ($N|a_s|/b_t = 0.012$), $n_c = 52$ for $N = 100$ ($N|a_s|/b_t = 0.058$), and $n_c = 88$ for $N = 900$ ($N|a_s|/b_t = 0.52$)]. The dashed line shows the Gross-Pitaevskii energy for $a_s/b = -0.5$. The $N|a_s|/b_t$ -axis above only applies to $a_s/b = -0.84$.
b) Mean square distance between the particles for the cases of a).

In the same figure we compare to results obtained with the present method for three different particle numbers. The interaction energies are remarkably similar to those of the stable mean-field solution where the scattering length in the Born approximation

equals the correct value. We also show the results of the less attractive zero-range interaction where the scattering length in the Born approximation is the same as for the finite range potential. Now the mean-field interaction energy is much less negative. We should emphasize that this comparison does not include the negative-energy states supported by the attractive pocket at short distance, see figure 5. They would appear below the “condensate-like” state shown in figure 6a.

Using equations (3) and (21) we compare in figure 6b $\langle r_{ij}^2 \rangle$ for the solutions of the mean-field approximation and the hyperspherical methods. The average distance is related to the interaction energy $E - E_0$. In a harmonic trap the relation $E_0 \propto \langle r^2 \rangle$ is valid. For condensates the trap determines the average properties. It is then not very surprising that the numerical calculations of $\langle r^2 \rangle$ show that the interaction energy roughly is proportional to the mean square radial difference between interacting and non-interacting systems, i.e., $E - E_0 \propto \langle r^2 \rangle - \langle r^2 \rangle_0$. The fact that these two sets of second moments are very close indicates that the corresponding wave functions also are similar.

Not surprisingly the mean square distance decreases with increasing particle number for all calculations with an attractive potential. As N approaches 1000 the Gross-Pitaevskii mean-field radius approaches zero due to the unavoidable collapse. The same behaviour is seen for radii and interaction energies, i.e., the average distance between particles decreases until the condensate collapses and the size vanishes in the mean-field while many-body bound states with smaller extension play a role in the hyperspherical description. Then also higher-order correlations can be expected to be essential and result in recombination processes.

For weak interactions or very small scattering lengths a stationary many-body state can be approximated by a product of single-particle amplitudes. However, stronger attraction between particles must invoke other degrees of freedom like clusterization. Then a simple single-particle description is not valid.

4.4. Validity conditions for the models

We want to compare validity criteria for our model and the mean-field approximation both for zero and finite-range interactions. We focus on the structure of a Bose-Einstein condensate where the wave function is located around the hyperradius $\rho \sim \sqrt{N}b_t$. Accurate angular eigenvalues in this region are therefore crucial for a proper description. If these hyperradii are sufficiently large, i.e., $\rho \sim \sqrt{N}b_t > N^{7/6}|a_s|$, the angular eigenvalue has reached its asymptotic value where $\lambda \approx \lambda_\delta$. This condition is equivalent to $N|a_s|/b_t < N^{1/3}$ which is obeyed by all stable condensates where $N|a_s|/b_t < 0.5 < N^{1/3}$ [14, 13].

The different models are valid if appropriately designed, i.e., our model should reproduce the correct scattering length whereas both the zero and finite-range mean-field interactions should reproduce this same correct scattering length but by using the Born approximation. The interaction energies and sizes would all be very similar

for the states corresponding to the condensate. To make this comparison and reach this conclusion we have to assume that the angular wave function is a constant (only *s*-waves) and the hyperradial function is equivalent to the single-particle product in mean-field computations. Otherwise the direct connection between wave functions and their properties is not possible. Fortunately, this connection is rather convincing as discussed in section 2. Furthermore this assumption about a specific form of the angular wave function is very similar to that of spherical Hartree-Fock computations for identical fermions.

If we for a given average hyperradius $\bar{\rho}$, through equation (3), relate the mean-field average distance \bar{r} by $\bar{r} \approx \bar{\rho}/\sqrt{N}$, then the density n of the system is given by

$$n \approx \frac{3}{4\pi\bar{r}^3} \approx \frac{3N^{3/2}}{4\pi\bar{\rho}^3}. \quad (60)$$

The zero-range mean-field method is usually claimed to be valid for condensates when $4\pi n|a_s|^3/3 \ll 1$, see [29, 5]. Then the number of particles within a scattering volume $4\pi|a_s|^3/3$ is on average much smaller than one.

On the other hand, in the zero-range asymptotic region of $\bar{\rho} > N^{7/6}|a_s|$ we have $n\bar{\rho}^3 > N^{7/2}n|a_s|^3$ immediately implying that $n|a_s|^3 < 1/N^2 \ll 1$, which means that the system is very dilute and both zero and finite-range mean-field energy is accurate.

For $\bar{\rho} < N^{7/6}|a_s|$ the large-distance asymptotics are not valid and the zero-range mean-field description breaks down. For $N^{1/2}|a_s| \ll \bar{\rho} < N^{7/6}|a_s|$ or equivalently $1/N^2 < n|a_s|^3 \ll 1$ the finite-range, but not the zero-range, mean-field is valid. For even smaller distances of $\bar{\rho} < N^{1/2}|a_s|$ also finite-range mean-field becomes invalid.

The present adiabatic hyperspherical method with two-body correlations explicitly allowed in the form of the wave function is first of all valid in the same region as the finite range mean-field approximation, i.e., for $N^{1/2}|a_s| < \bar{\rho}$, where correlations are expected to be insignificant. However, the validity range of the hyperspherical method with two-body correlations incorporated extends to hyperradii smaller than $N^{1/2}|a_s|$, where two-body correlations are sufficient to describe the clusterizations.

When higher-order clusterizations occur, any method without correlations higher than two-body must break down. The density when this happens for this hyperspherical method is not easily derived. The lower limit is probably when the distance between two particles on average equals the interaction range b , i.e., $N^{1/2}b < \bar{\rho}$. However, for nuclei with identical fermions the radius at saturation is about $N^{1/3}b$ where the mean-field approximation is very successful. This limit would then correspond to $N^{5/6}b < \bar{\rho}$, but identical boson systems may allow even smaller hyperradii.

In conclusion, the validity regions for the two-body correlated method (hyperspherical), finite-range methods (finite-range mean-field and hyperspherical), and the zero-range mean-field are estimated to be

$$\bar{\rho} > \sqrt{N}b \quad \text{for two-body correlated method,} \quad (61)$$

$$\bar{\rho} > \sqrt{N}|a_s| \quad \text{for finite-range methods,} \quad (62)$$

$$\bar{\rho} > N^{7/6}|a_s| \quad \text{for finite- and zero-range methods.} \quad (63)$$

These relations can with equation (60) be expressed via the density

$$n|a_s|^3 < \left(\frac{|a_s|}{b}\right)^3 \quad \text{for two-body correlated method,} \quad (64)$$

$$n|a_s|^3 < 1 \quad \text{for finite-range methods,} \quad (65)$$

$$n|a_s|^3 < \frac{1}{N^2} \quad \text{for finite- and zero-range methods.} \quad (66)$$

When the density is low all the three approximations are valid and the energies are very similar. This of course assumes that the renormalization is appropriate. For higher densities the importance of correlations increases and the mean-field approximations break down. At some higher density also two-body correlations are insufficient and the particles may want to exploit higher-order correlations. In any case, the wave functions can not be better than the Hilbert space they span, no matter how precise the energy is computed.

5. Summary and conclusion

The method of hyperspherical adiabatic expansion is briefly sketched for a system of identical bosons. The form of the wave function is chosen as the s -waves in a partial wave expansion of the Faddeev-Yakubovskii cluster amplitudes. This restriction is expected to be accurate for large distances and dilute systems. We relate to the Jastrow ansatz designed to deal with correlations in rather dense systems. We discuss the theoretical connections between all these approaches and the mean-field approximation both with zero and finite-range interactions.

The angular eigenvalues in the hyperspherical adiabatic expansion appear as crucial ingredients in the radial potentials. We use the analytic expressions recently parametrized to reproduce the results of full numerical computations. We first discuss the general properties of these eigenvalues as functions of hyperradius for arbitrary particle number and arbitrary scattering length. The large-distance behaviour corresponding to the zero-range mean-field result is obtained.

The radial potential has a minimum at large distance when particle number times scattering length divided by trap length is less than about 0.5. The wave function of the condensate is located in this minimum. In addition, for sufficiently large scattering lengths an intermediate region appears with a radial potential decreasing inversely proportional to the square of the hyperradius. This region supports the many-body Efimov-like states. At much smaller distances a pronounced attractive pocket is present when the two-body potential is attractive. We give analytical estimates of the number of bound states located in these different regions. We then discuss the decay properties eventually arising from recombination processes. In particular the highest-lying Efimov-like states located at large distances recombine corresponding to widths much smaller than the level spacing. These peculiar states could then leave observable traces.

Finally, we discussed the connection between this work and the mean-field approximation. We first emphasized that the effective two-body interactions must

be related to the Hilbert space for the wave function. We specify the necessary renormalization for the mean-field restriction. Numerical comparison for energies and radii are then presented. The validity conditions for the models are discussed and expressed as regions in hyperradius. These regions increase from zero via finite-range mean-field approximation to the hyperspherical adiabatic expansion method.

Most of the results are independent of the structure of the two-body interaction. The conclusions are derived in terms of scattering length, number of particles, external field frequency and occasionally the effective range of the two-body potential.

- [1] M. H. Anderson *et al.*, *Science* **269**, 198 (1995).
- [2] C. C. Bradley, C. A. Sackett, J. J. Tollett, and R. G. Hulet, *Phys. Rev. Lett.* **75**, 1687 (1995).
- [3] K. B. Davis *et al.*, *Phys. Rev. Lett.* **75**, 3969 (1995).
- [4] C. J. Pethick and H. Smith, *Bose-Einstein Condensation in Dilute Gases* (Cambridge University Press, Cambridge, 2001).
- [5] L. Pitaevskii and S. Stringari, *Bose-Einstein Condensation* (Clarendon Press, Oxford, 2003).
- [6] E. Timmermans, P. Tommasini, M. Hussein, and A. Kerman, *Phys. Rep.* **315**, 199 (1999).
- [7] E. A. Donley *et al.*, *Nature (London)* **412**, 295 (2001).
- [8] S. K. Adhikari, *Phys. Rev. A* **66**, 013611 (2002).
- [9] S. K. Adhikari and P. Muruganandam, *J. Phys. B* **35**, 2831 (2002).
- [10] E. Timmermans *et al.*, *Phys. Rev. Lett.* **83**, 2691 (1999).
- [11] E. A. Donley, N. R. Claussen, S. T. Thompson, and C. E. Wieman, *Nature (London)* **417**, 529 (2002).
- [12] D. Blume and C. H. Greene, *Phys. Rev. A* **66**, 013601 (2002).
- [13] J. L. Roberts *et al.*, *Phys. Rev. Lett.* **86**, 4211 (2001).
- [14] J. L. Bohn, B. D. Esry, and C. H. Greene, *Phys. Rev. A* **58**, 584 (1998).
- [15] O. Sørensen, D. V. Fedorov, and A. S. Jensen, *Phys. Rev. Lett.* **89**, 173002 (2002).
- [16] O. Sørensen, D. V. Fedorov, and A. S. Jensen, *Phys. Rev. A* **66**, 032507 (2002).
- [17] O. Sørensen, D. V. Fedorov, and A. S. Jensen, e-print cond-mat/0305040, submitted to *Phys. Rev. A*.
- [18] N. Barnea, *Phys. Lett. B* **446**, 185 (1999).
- [19] O. Sørensen, D. V. Fedorov, A. S. Jensen, and E. Nielsen, *Phys. Rev. A* **65**, 051601 (2002).
- [20] B. H. Bransden and C. J. Joachain, *Physics of atoms and molecules* (Longman Scientific & Technical, USA, 1983).
- [21] L. D. Faddeev, *J. Exptl. Theoret. Phys. (U.S.S.R.)* **39**, 1459 (1960) [Sov. Phys. JETP **12**, 1014 (1961)].
- [22] O. A. Yakubovskii, *Yad. Fiz.* **5**, 1312 (1967) [Sov. J. Nucl. Phys. **5**, 937 (1967)].
- [23] L. D. Faddeev and S. P. Merkuriev, *Quantum Scattering Theory for Several Particle Systems* (Kluwer Academic, Dordrecht, 1993).
- [24] F. Ciesielski and J. Carbonell, *Phys. Rev. C* **58**, 58 (1998).
- [25] I. Filikhin and A. Gal, *Nucl. Phys. A* **707**, 491 (2002).
- [26] A. Bijl, *Physica* **7**, 869 (1940).
- [27] R. B. Dingle, *Phil. Mag.* **40**, 573 (1949).
- [28] R. Jastrow, *Phys. Rev.* **98**, 1479 (1955).
- [29] S. Cowell *et al.*, *Phys. Rev. Lett.* **88**, 210403 (2002).
- [30] D. V. Fedorov and A. S. Jensen, *Phys. Rev. Lett.* **71**, 4103 (1993).
- [31] A. S. Jensen, E. Garrido, and D. V. Fedorov, *Few-Body Syst.* **22**, 193 (1997).
- [32] N. N. Khuri, A. Martin, and T.-T. Wu, *Few-Body Syst.* **31**, 83 (2002).
- [33] E. Nielsen, D. V. Fedorov, A. S. Jensen, and E. Garrido, *Phys. Rep.* **347**, 373 (2001).

- [34] S. L. Cornish *et al.*, Phys. Rev. Lett. **85**, 1795 (2000).
- [35] B. D. Esry and C. H. Greene, Phys. Rev. A **60**, 1451 (1999).
- [36] D. V. Fedorov and A. S. Jensen, Phys. Rev. A **63**, 063608 (2001).